Vol. 2 No. 3 (2024)

Spectrum of Engineering Sciences

Online ISSN
3007-3138
Print ISSN
3007-312X

Design of a Novel Quazi-Elliptic RF Bandpass Filter Using Antiparallel Coupled Lines for Sub 6 GHz 5G Band

Irsa Jamil Bajwa
MS, (Electrical Engineering), Electrical Engineering Department, Riphah International University, Islamabad, Pakistan.
Email: wxyirsa@gmail.com
Dr. Sohail Khalid
Associate Professor, Head of Electrical Engineering Department, Faculty of Engineering & Applied Sciences, Riphah International University, Islamabad, Pakistan.
Email: sohail.khalid@ieee.org

Abstract

This study develops a compact microstrip bandpass filter using a modified coupled line structure. By adjusting the coupled line step split ratio, the finite frequency transmission zero can be tuned. The passband produces two transmission zeros. Designing and evaluating the suggested filter makes use of HFSS and ADS. Two prototypes are produced on the Roger Duriod 5880. The fabrication losses are adjusted by post-fabrication tuning. A vector network analyzer is used to do the measurement. The output prototype size is 0.2λg x 0.18λg. The findings of the simulated and measured S-parameters are in good agreement.

Keywords: Bandpass filter, modified coupled-line structure, compact filter design, miniaturized filter, wireless communication, out-of-band rejection, high performance filter.

1. Introduction

A two-port, reciprocal, passive, linear device called a microwave filter greatly attenuates undesirable signal frequencies while allowing transmission of desired frequencies. In broad terms, insertion loss, return loss, frequency selectivity (or attenuation at the rejection band), group delay variation in the pass band, and other terminology are used to characterize the electrical performance of the filter. Small insertion loss, high return loss, and high frequency selectivity are necessary for filters to have good impedance matching with associated components and to avoid interference. In order to keep up with this development, RF front ends typically need band pass filters with a fair degree of bandwidth. The band pass filter is a crucial element in microwave communication systems and is typically used in both receivers and transmitters [1].

Furthermore, the compactness, high selectivity, and convenience of fabrication of the microstrip-based filters make them one of the most prominent structures. Numerous researchers have focused on single-band, double-band, and broadband bandpass filter topologies up to this point. [2]. A dual band filter can be employed in place of two separate single bandpass filters in a single transceiver system that operates in two frequency bands in order to reduce the level of volume. Cross-coupled resonators may be used to provide a transmission zero in the middle of a wide bandpass or an embedded bandstop filter can be used inside the wideband band pass filter to achieve dual band operation [2].

This work uses a single switchable J-inverter to demonstrate a unique switchable dual-/single band switchable bandpass filter. The single J-inverter with switches makes it simple to change the suggested filter design from a two-pole dual-passband mode to a four-pole single-passband mode. This is accomplished by

employing a new hybrid resonator configuration with a dual-band bandpass filter, which consists of a J-inverter and two parallel resonators. A high stopband attenuation level is obtained due to a transmission zero between the two passbands, as well as two bandwidths and two center frequencies of the dual-passband mode [3]. The physical implementation of an innovative ultra-wideband microstrip filter is proposed. The short-circuited stubs with etched rectangular lattice are the intended target for the band pass filter. Better return loss is provided by the etching. The lowered stop-band characteristics are realized using the quarter-wavelength short-circuited stubs [4]. This work presents an open and short circuited stub micro strip ultra-wideband (UWB) band pass filter. Four coupled-line stubs—three short and one open—are used to create the suggested filter. The whole UWB pass band, which ranges from 3.05 GHz to 10.6 GHz, is covered by this filter. The design was accurately calculated, and CST software was used for design simulation to assess performance [5].

This study presents and experimentally validates an ultra-wideband microstrip bandpass filter (BPF), which runs from 2 GHz to 4.7 GHz, with good selectivity and wide rejection band. The filter is made up of microstrip lines with shorted stubs on the top side working as a high pass filter (HPF) and defected ground structures (DGSs) in the shape of dumbbells on the bottom side functioning as a low pass filter (LPF). The created hybrid circuit is a low-cost, production-friendly bandpass filter with controllable pass- and rejection-band characteristics [6]. It is suggested to use two pairs of antiparallel mixed-coupled stepped-impedance resonators (SIRs) in a fourth-order microstrip quazi-elliptic BPF. It improves the accuracy of obtaining the necessary frequency responses and lessens parasitic interaction between nonadjacent resonators [7]. A technique for creating microstrip bandpass filters that have wide

stopbands, UWB performance, and practical dimensions is provided. The suggested technique involves joining three subsections with various lengths and coupling factors to create a stepped-impedance parallel-coupled microstrip design. The ideal length and coupling factor for each of those subsections for a UWB passband and suppressed second and third harmonic responses in the stopband are determined using a theoretical model that is developed. Three transmission zeros in the upper stopband and three transmission poles in the passband are generated and properly positioned to achieve the desired performance.

The developed model demonstrates that the three-subsection coupled structure's overall length is equal to one-third of the effective wavelength at the passband's center [8]. It is suggested that coupled-line coupling structures be used to create quasi-elliptic bandpass filters (BPFs). One pair of symmetrical transmission zeros are introduced by the coupled line structure, which serves as the input coupling structure for a BPF, at around the cutoff frequencies. In light of this, this study makes a significant effort to build the coupling structure's equivalent circuit. A fundamental building component for the design of quasi-elliptic BPFs is the coupling structure. The theoretical and practical research shows that a Chebyshev filter can be converted into a quasi-elliptic filter by use of the coupling structure [9].

In this study, a small microstrip bandpass filter is designed using a modified coupled line structure. For improving frequency response, modified coupled line design components were presented and analyzed. The modified coupled line structures are simulated and validated in the first portion using ADS. The modified coupled line structure is validated in the next step using HFSS. It explain the findings of the full-wave EM simulation of the layout, the microstrip-based filter, and the ideal transmission line

filter. In addition, an analysis is done on the proposed topology's current distribution and ideal S-parameter response when the electrical length is changed. Through fabrication and testing, both designs of the modified coupled line structures are validated. The microstrip design is created with Roger Duroid 5880. On a network analyzer, the testing is carried out. The simulated prototypes and both actual ones are measured and compared.

2. Design Procedure and Topology

The presented design focuses on a novel modified coupled line structure with an open circuit stub, short circuit stub at one end, two coupled lines with varying spacing, and various coupled lines with different widths on the other. In this arrangement, the structure offers a response similar to that of a conventional coupled line structure, but with better selectivity and more transmission zeros at finite frequencies. Fig. 1 depicts the suggested unit element of a modified coupled line structure. The midpoint of the structure is where it splits off first.

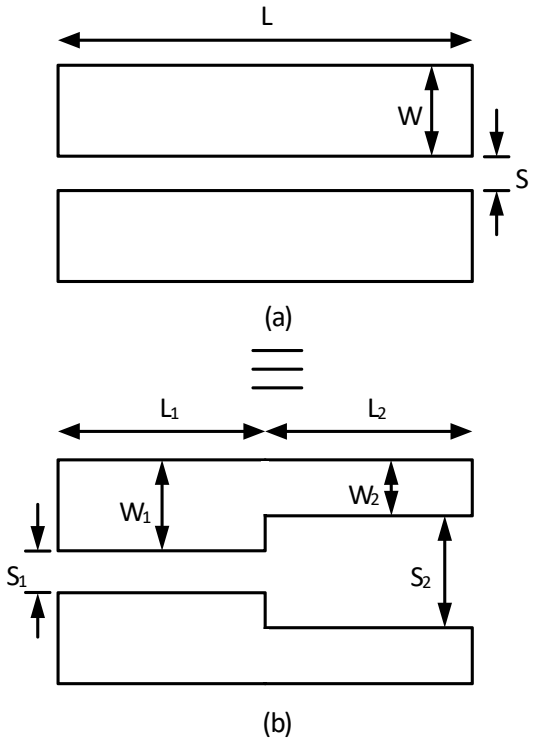

Figure 1: (a) Conventional Coupled line structure
(b) Proposed modified coupled line structure

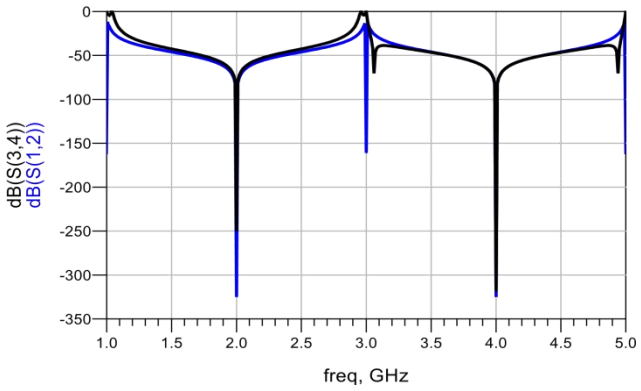

Fig. 2: Frequency response of the conventional and proposed coupled line structure.

Figures 3, 4, and 5 depict the examination of coupled line structures with various splitting lengths. According to the coupled line splitting lengths, the finite frequency transmission zero close to the passband can be tuned.

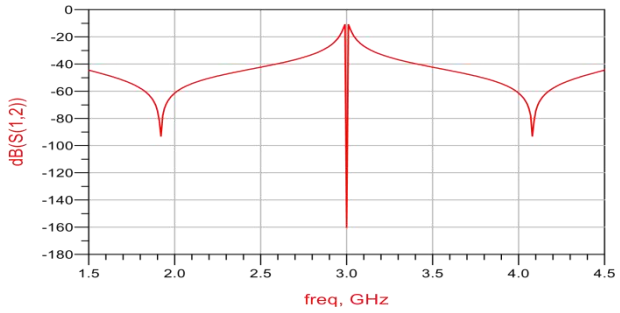

Figure 3: Frequency response of the proposed coupled line structure with 30-60 split

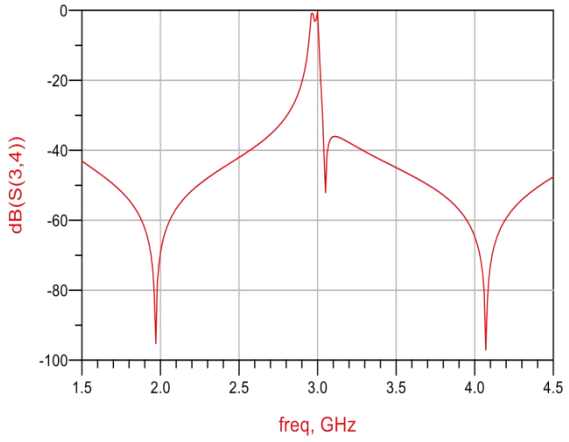

Fig. 4: Frequency response of the proposed coupled line structure with 40-50 split

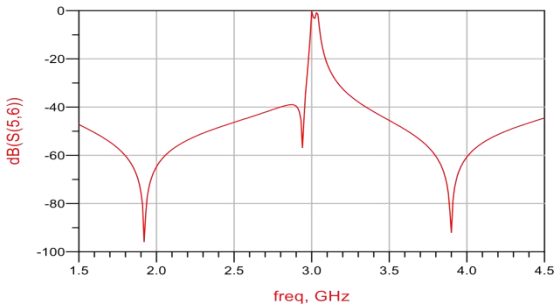

Fig. 5: Frequency response of the proposed coupled line structure with 10-80 split

Fig. 6 illustrates the design topology of a bandpass filter using a distributed equivalent circuit model and a modified coupled line structure. A modified coupled line with an open stub at one end and a short circuit stub at the other makes up the circuit. Both connected line circuits' even-odd mode impedances are displayed together with the corresponding electrical lengths. Employing the proposed circuit's overall transfer matrix, the filtering function may be determined. The distributed equivalent circuit can be used for evaluating the transfer matrix. The overall transfer matrix is shown in Eq. 2.1, and each section's transfer matrix is indicated by an associated subscript. To get the entire transfer matrix, multiply each component that cascaded. The parameters of the transfer matrix in Eq. 2.2 are related to the transfer function S12. Eq. 2.3 [10] can be used to compute the filtering function once the S12 has been determined. Two transmission poles and one transmission zeros that are near to the passband are provided by the bandpass filter in this configuration.

$$[T_{total}] = [Tocse].[Tocsh].[Tocse].[Tcl].[Tscsh].[Tscse].[Tscsh] \quad (2.1)$$

$$[t_{total}] = \begin{bmatrix} A & B \\ C & D \end{bmatrix} \quad (2.2)$$

$$S_{21} = \frac{2}{A+B+C+D} \quad (2.3)$$

$$|S_{21}(j\omega)|^2 = \frac{1}{1+\varepsilon^2 G_N^2(\theta)} \qquad (2.4)$$

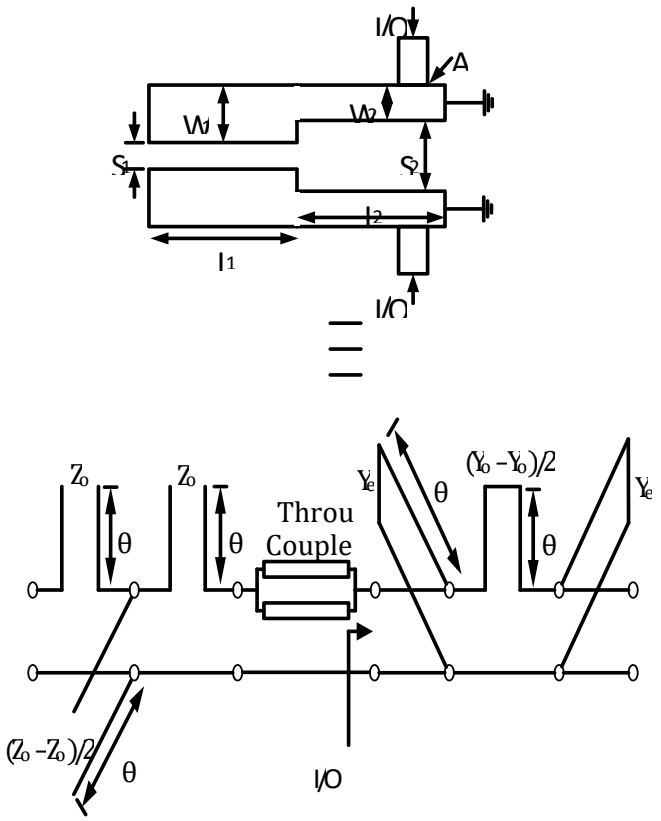

Fig. 6: Topology of Proposed bandpass filter using modified coupled line and its distributed equivalent circuit model.

3. Design Procedure of Bandpass Filter Using Modified Coupled Line Structure on Ads / Ads Procedure on Bandpass Filter Using MCL Structure

Fig. 7 depicts the HFSS structure with air acting as a box. In order to deliver the signal for the simulation, lumped ports are allocated to the circuit design, which is suspended in the air. The air has been given its radiation boundary conditions. The substrate is Roger Duriod 5880, which has a height of 0.787 mm and εr value of 2.2. The diameter of the via hole is 1mm. The first coupled line structure's parameters are W1=1.5mm, L1=3.5mm, and S1=0.2mm, whereas the second coupled line structure's values are W2=1mm, L2=13mm, and S2=0.95mm. With the solution frequency set at 4 GHz, the sweep frequencies for the simulation are set at 1 to 8 GHz.

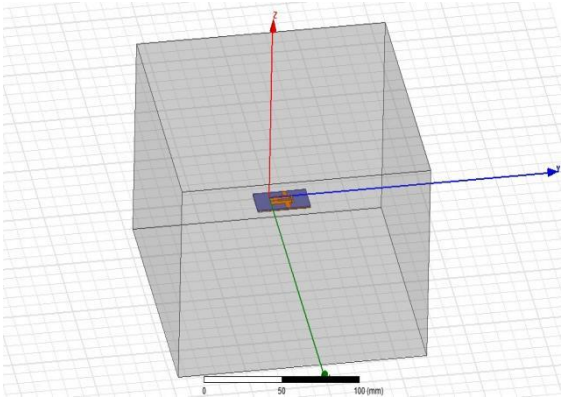

Fig. 7: Design enclosed in the air with half wavelength clearance.

Fig. 8 depicts the layout design together with all design parameters. The input/output signal is injected from the side of coupled lines for design compactness. The size of the circuit is 0.2λg x 0.18λg. A parametric analysis and optimization can be performed on the circuit in order to find the optimal solution.

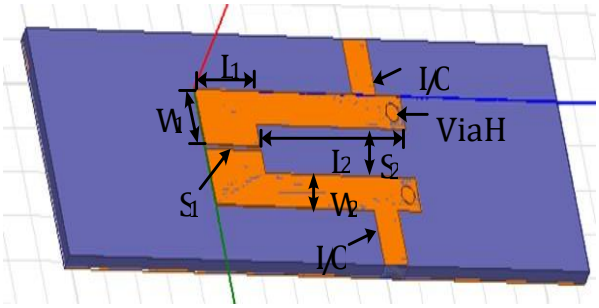

Fig. 8: HFSS bandpass filter design on Microstrip substrate

4. Design Procedure of Bandpass Filter Using Modified Coupled Line Structure on HFSS/ HFSS Procedure on Bandpass Filter Using MCL Structure

In order to analyze the design for the ideal response, it is also simulated in ADS. The ideal electrical parameters are transformed into physical parameters using a line calculator. Since the ideal design does not result in any losses, the acquired results cannot be used for fabricating the prototype. The loss in the intended circuit must be realized by a microstrip conversion.

The microstrip structure with globally defined variables is seen in Fig. 9. The extra loss caused by the microstrip in the

design can be eliminated by tuning and optimization. The minimum limit for fabrication is 200 microns.

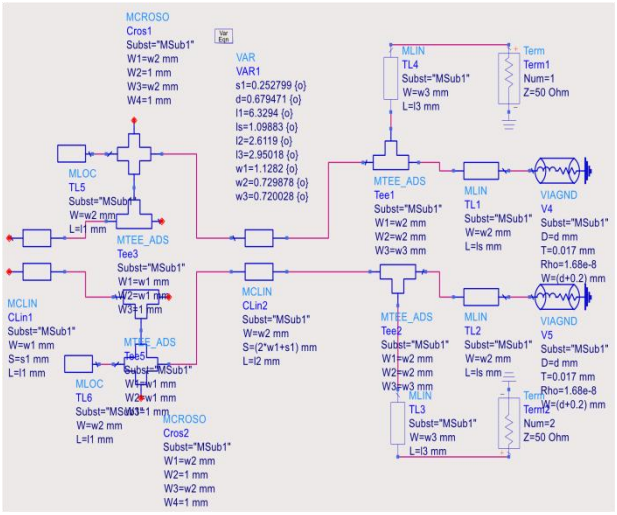

Figure 9: Microstrip schematic design of proposed bandpass filter

For precise modeling and analysis of high-frequency circuits and systems, ADS with full-wave electromagnetic simulation is used. The layout design seen in Fig. 10 was produced using the microstrip simulated circuit. On transmission lines TL1 and TL2, respectively, the via holes are produced. Ports are assigned to TL3 and TL4, and a mesh with 20 cells per wavelength is produced. The sweep frequency used to build the simulation setup ranges from 1 GHz to 8 GHz.

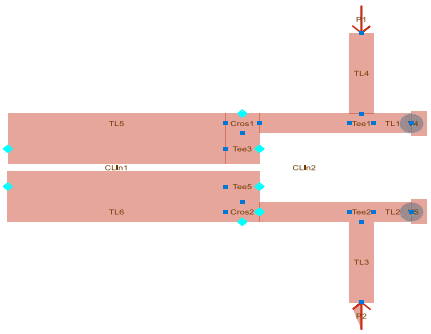

Figure 10: Design layout in ADS momentum

The Co-Simulation Optimization setup is shown in Fig. 11. For each full-wave layout simulation, the optimizer runs and returns the error factor. Once the required outcome has been obtained, the ADS momentum design is next simulated with a

mesh size of 80 cell/wavelength using the same optimized parameter values. A Gerber file is created for fabrication after receiving a satisfactory response.

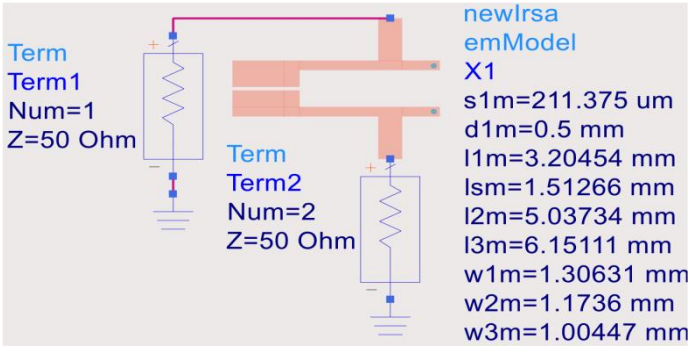

Figure 11: Co-Simulation Optimization in ADS

In addition, the layout design is depicted in Fig. 12 and includes a bandpass filter with an operating frequency of 1.1 GHz and out-of-band suppression of 40dB up to 7 GHz. This filter transitions from a high-impedance coupled line to a low impedance coupled line using a tapered line.

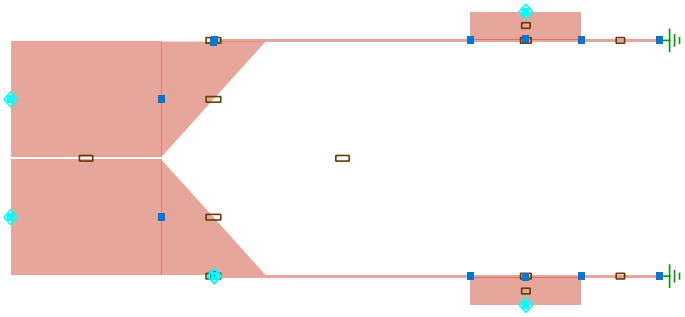

Figure 12 : Design layout in ADS momentum

5. Results

The proposed topology has a 2.2 electric permittivity and is designed on Roger Duriod 5880. Figure 13 depicts the design filter's simulated frequency response. With 3.8 GHz as its center point, a bandpass with a fractional bandwidth of 6.8% is achieved. In the passband, two transmission poles are obtained. A single transmission zero at 2.83 GHz is achieved, improving selectivity. The insertion loss S12 at center frequency is 1.28 dB, and the return loss S11 is below 10 dB. The parametric analysis of the suggested

design is shown in Fig. 14. It is clear that the design S-parameter response is being affected by variations in electrical length and even odd mode impedances. The optimal filter parameters have been chosen for microstrip fabrications after parametric analysis.

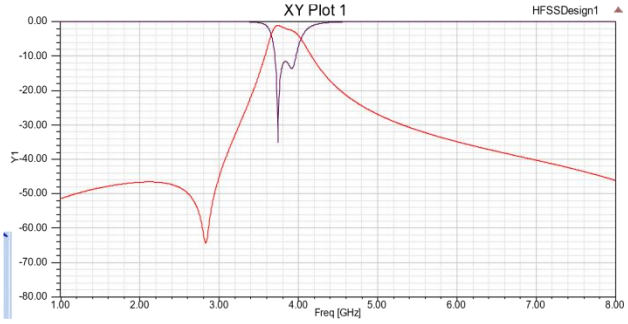

Fig. 13: S-parameters response of a proposed bandpass filter

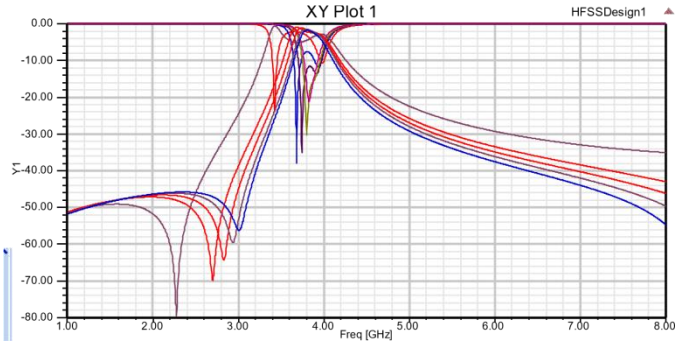

Fig. 14: S-parameters response of parametric sweep for various filter parameter combinations

The ADS schematic is designed using an ideal circuit to validate the distributed equivalent circuit model. The ideal S-parameter frequency response in Fig. 15 displays two transmission zeros at finite frequencies. Because one of the transmission zeroes is so near to the passband, it is appropriate for applications requiring an asymmetrically highly selective frequency response.

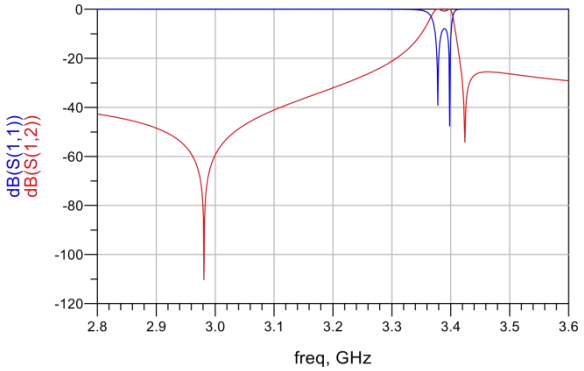

Fig. 15: Ideal S-parameters response on ADS

Using a line calculator, the ideal circuit parameters are transformed into physical line parameters. With εr=2.2, the tangent loss is 0.0009. On both sides of the substrate, a 17 micron copper cladding is present. Although optimization and tuning have been carried out in order to improve the results, the initial results do not map to the requirements. In Fig. 16, the simulated S-parameters are displayed. With a fractional bandwidth of 6.8%, the return loss S11 is below 10 dB and is centered at 3.8 GHz.

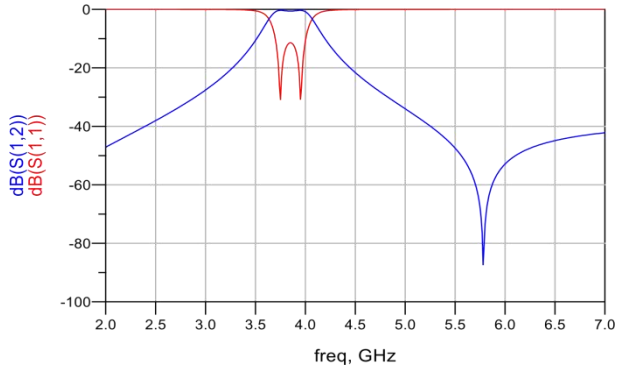

Fig. 16: S-parameter frequency response of microstrip design

Before the fabricating, full wave EM simulations were conducted. The schematic has been used to produce the layout design. The ports are indicated in the momentum layout design, and via holes are realized through the substrate from the top conductor to the ground. The mesh size is initially set to 20 mesh/wavelength. Fig. 17 displays the full-wave EM simulations' S-parameter frequency response. The shown response exhibits a few discrepancies brought on by substrate, dielectric, and conduction losses. Co-simulation optimization is used to reduce response inconsistency. The schematic window uses the generated filter design symbol for tuning and optimization. Fig. 18 depicts the resultant frequency response following optimization.

Prior to extracting the Gerber file, the 80 mesh/wavelength is chosen to provide most accuracy. To reduce soldering mismatch

losses, copper is inserted into the single via hole. The trace must be at least 0.2mm long. Figure 19 depicts the finalized design layout.

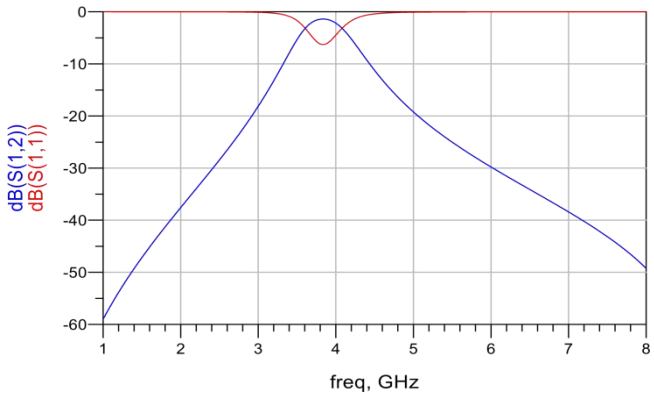

Figure 17: S-parameter response of Full wave EM simulations

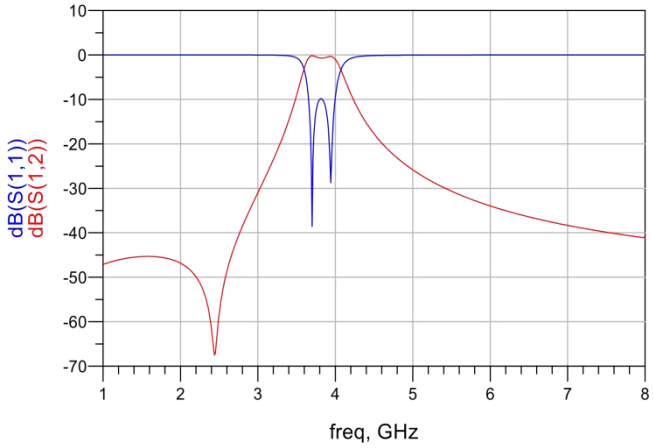

Fig. 18: S-parameter response of Full wave EM simulations after Co-simulation optimization

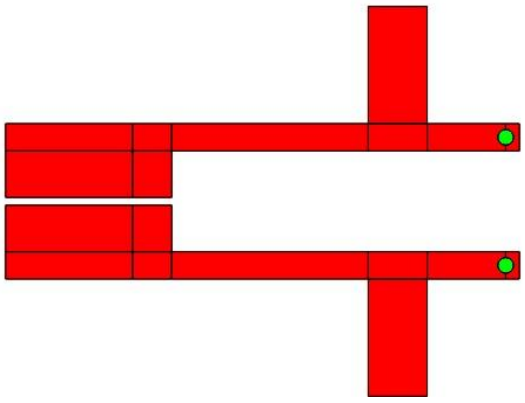

Fig. 19: Gerber layout design with two via holes

Further research is conducted to get a wide out-of-band rejection using the same modified coupled line topology. For this,

a coupled line structure with a high impedance is employed with a tapered line. The acquired band at 1.1 GHz with two transmission poles has an out-of-band rejection level below 40 dB up to 7 GHz. Fig. 20 displays the simulated S-parameter response. At 6.9 GHz, a finite frequency transmission zero is visible.

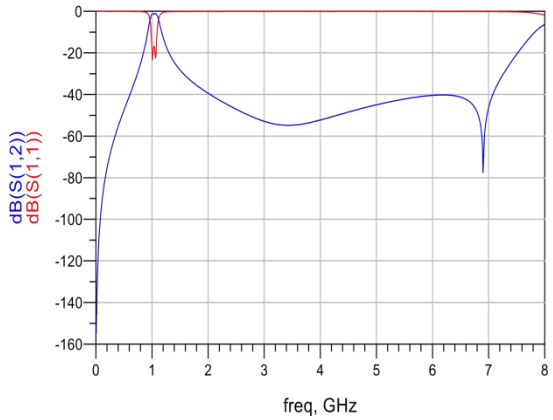

Fig. 20: S-parameter frequency response of bandpass filter

After obtaining the results of the ADS EM simulation, the current distribution at three frequencies is analyzed. Figure 21 (a), (b), and (c) illustrate the current distribution at 2.1 GHz, 3.61 GHz, and 6.6 GHz, respectively. The active circuit can be seen in the passband at 3.61 GHz, but only port one is active at 2.1 GHz and 6.6 GHz. This indicates that the reflection loss is considerable at these frequencies, making transmission impossible.

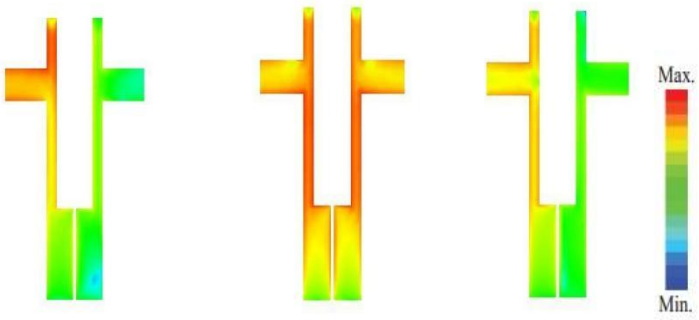

(a) 2.1 GHz (b) 3.61 GHz (c) 6.6 GHz

Fig. 21: Current distribution of proposed bandpass filter

Two prototypes are fabricated on the microstrip substrate Roger Duroid 5880 to validate the proposed design. The fabricated prototypes are shown in Figs. 22 and 23. The copper filling of the

via holes will assist to reduce soldering mismatch during measurements. At the I/O ports, SMA connecters are utilized for measurement. For both fabricated prototypes, the S-parameter is measured using a vector network analyzer.

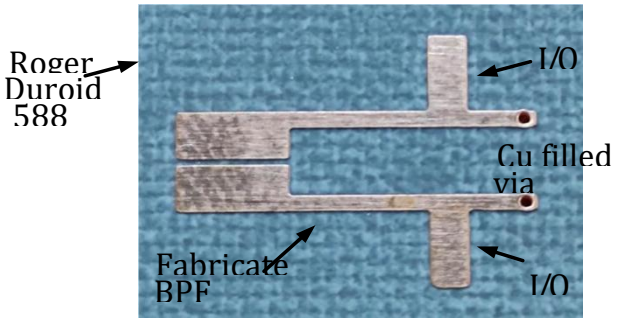

Fig. 22: Fabricated Prototype of proposed BPF using modified coupled line

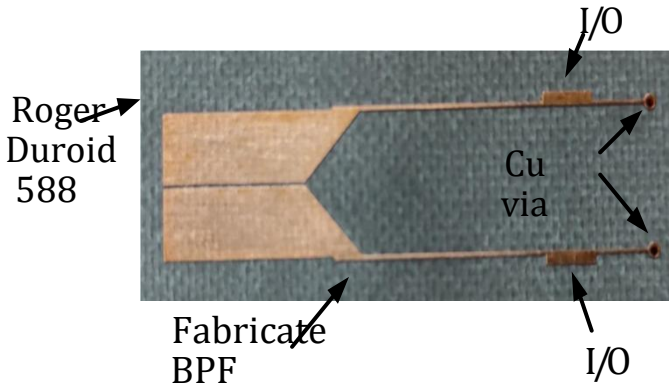

Fig. 23: Fabricated Prototype of BPF with high out-of-band rejection

Using an Agilent N5242A vector network analyzer, both fabricated prototypes were measured. The frequency range for the sweep is 0 GHz to 8 GHz. Figure 24 shows the measured result of the bandpass filter's first fabricated prototype. In the passband with a fractional bandwidth of 6.8% and a centered frequency of 3.8 GHz, two transmission poles are obtained. From 0 to 3.5 GHz, out-of-band rejection is less than 10 dB, but from 4.2 GHz to 8 GHz, it is greater. 2.44 GHz has one finite frequency transmission zero and -67 dB of rejection. There are a few discrepancies between results from simulations and measurements. This response

discrepancy is the result of a soldering-related I/O port mismatch. Both the in-band reflection and the insertion loss are under 1 dB. The prototype is simple to fabricate and is compact (0.2λg x 0.18λg).

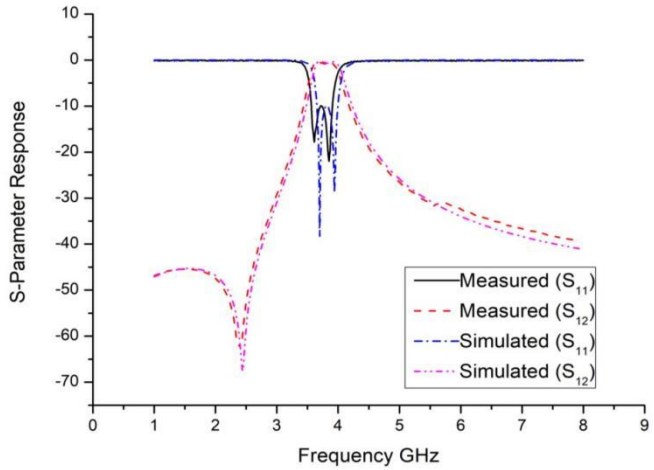

Fig. 24: Simulated and measured S-Parameter response comparison of first prototype

Fig. 25 displays the second prototype's measured result. 20 dB rejection is used to provide a wide out-of-band response from 1.55 GHz to 8 GHz. At 6.3 GHz, a finite frequency transmission zero is attained. The zoomed-in band frequency response with two transmission poles and a fractional bandwidth of 18% is displayed in a sub-figure that is centered at 1.1 GHz. In wireless communication systems where out-of-band rejection is crucial, this sort of frequency response is ideal. The measured and simulated responses are closely correlated.

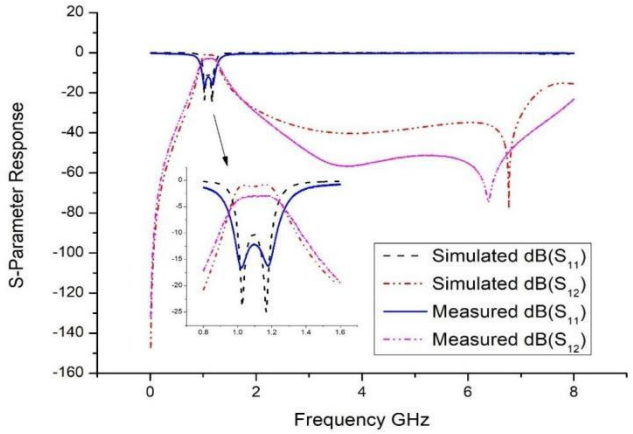

Fig. 25: Simulated and measured S-Parameter response comparison of second prototype

Table 1: Comparison Table

Comparison of the presented work with already published work.

Ref #	Center Frequency (GHz)	Insertion loss (dB)	Return loss (dB)	Size (λg * λg)	Out of band Rejection @	Fractional Bandwidth (%)
[1]	20	<0.9	>8.8	N/A	21.2 -24 GHz @30dB	10
[2]	5.85/6.85	<2.2	>20	N/A	6.2-7 GHz @35dB	1.3
[3]	0.8/1	<4.9	>15	N/A	1-1.4GHz @15dB	1.5
[7]	1.65	<1.7	>16	0.64x0.48	1.65-1.85GHz @60dB	6
[9]	2	<1.7	>17	0.79x0.06	2.2-3GHz @30dB	11
[11]	6.25	<1.07	>17.5	N/A	7-10GHz @10dB	18.9
[12]	2.9	<1.14	>12	N/A	3-3.4GHz @10dB	6.8
[13]	2.1	<1.1	>20	0.76x0.62	2.5-6.5GHz @20dB	16.6

This Work D_1	**1.1**	**<1**	**>11**	**0.2x0.18**	**0-3.5GHz @10dB 4.2-8 GHz @10dB**	**6.8**
This Work D_2	**3.8**	**<1.5**	**>10**	**0.22x0.04**	**1.55-8GHz @20dB**	**18**

The proposed bandpass filter using a modified coupled line, offers higher electrical performance while retaining a compact size and simplicity in fabrication. The filter design parameters are altered to achieve the out-of-band rejection. Further research into this unit cell is possible in order to increase the passband's transmission pole count and get higher bandwidths.

6. **Conclusion**

A modified couple-line structure-based bandpass filter has been proposed in this article. A step-impedance coupled line makes up the circuit topology. The location of transmission zero depends on the split percentage in the coupled line. A highly coupled open circuit stub and a weakly coupled short-circuited stub separates the through-coupled line. The input/output is positioned close to the short-circuited stub to retain compactness. The step impedance resonator's intrinsic feature causes a 20% reduction in line length, further enhancing compactness. The suggested bandpass filter generates a two-pole bandpass response with a fractional bandwidth of 6.8%, centered at 3.8 GHz, in this arrangement. For improved selectivity and out-of-band rejection, one finite frequency transmission zero is obtained. When the in-band insertion loss is less than 0.9 dB and the in-band reflection loss is less than 10 dB, the suggested filter design offers

good electrical performance. The size of the circuit is 0.2λg x 0.18λg. The findings from simulations and measurements are well correlated. In addition, a wideband out-of-band rejection is obtained by modifying the physical parameters of a suggested filter. With 1.1 GHz as the central frequency, this design produced two transmission poles in the passband with a fractional bandwidth of 18%. At 7 GHz, the finite frequency transmission zero is achieved. The reflection loss is under 11 dB, while the insertion loss is under 1 dB. The size of the circuit is 0.22λg x 0.04λg. The observed results and full wave EM simulations are in good agreement.

Further research into this unit cell has the potential to increase the number of transmission poles inside the passband, which would ultimately result in the acquisition of wider bandwidths and higher selectivity. To achieve improved passband to stopband roll-off and out-of-band rejection, the suggested coupled line structure can be investigated further and incorporated into other design topologies.

7. References

[1] Sabat, R. R., & Karan, C. DESIGN & OPTIMIZATION OF MICROSTRIP PARALLEL COUPLED BANDPASS FILTER AT 20 GHZ.

[2] Rezaee, M., & Attari, A. R. (2014, October). A novel dual mode dual band SIW filter. In *2014 44th European Microwave Conference* (pp. 853-856). IEEE.

[3] Cho, Y. H., Park, C., & Yun, S. W. (2021). 0.7-1.0-GHz switchable dual-/single-band tunable bandpass filter using a switchable J-Inverter. *IEEE Access*, *9*, 16967-16974.

[4] Singhal, P. K., Mathur, S., & Baral, R. N. (2011). Ultra-wide microstrip band pass filter using short circuited stubs. *Journal of Electrical and Electronics Engineering Research*, *3*(6), 101-107.

[5] Gupta, P., & Bhatia, D. (2014, November). Ultra-Wideband Bandpass Filter Using Coupled Line Stubs. In *2014 International Conference on Computational Intelligence and Communication Networks* (pp. 126-128). IEEE.

[6] Keskin, A. K., & Partal, H. P. (2012, September). An UWB high-q bandpass filter with wide rejection band using defected ground structures. In *2012 IEEE International Conference on Ultra-Wideband* (pp. 99-102). IEEE.

[7] Zakharov, A., Rozenko, S., Pinchuk, L., & Litvintsev, S. (2021). Microstrip quazi-elliptic bandpass filter with two pairs of antiparallel mixed-coupled SIRs. *IEEE Microwave and Wireless Components Letters*, *31*(5), 433-436.

[8] Abbosh, A. M. (2011). Design method for ultra-wideband bandpass filter with wide stopband using parallel-coupled microstrip lines. *IEEE Transactions on microwave theory and techniques*, *60*(1), 31-38.

[9] Chen, C. J. (2018). A coupled-line coupling structure for the design of quasi-elliptic bandpass filters. *IEEE Transactions on Microwave Theory and Techniques*, *66*(4), 1921-1925.

[10] Hunter, I. (2001). *Theory and design of microwave filters* (No. 48). Iet.

[11] Zhang, W., Ding, S., Huang, Y., Zhu, Z., He, W., & Bozzi, M. (2023). Planar single-/dual-band bandpass filters based on new perturbed multi-mode SIW circular cavity. *Journal of Electromagnetic Waves and Applications*, *37*(3), 323-334.

[12] Zhang, Y., Zhang, X. Y., Gao, L., Gao, Y., & Liu, Q. H. (2019). A two-port microwave component with dual-polarized filtering antenna and single-band bandpass filter operations. *IEEE Transactions on Antennas and Propagation*, *67*(8), 5590-5601.

[13] Iqbal, A., Tiang, J. J., Wong, S. K., Wong, S. W., & Mallat, N. K. (2021). QMSIW-based single and triple band bandpass

filters. *IEEE Transactions on Circuits and Systems II: Express Briefs*, *68*(7), 2443-2447.